JGP Journal of General Physiology

METHODS AND APPROACHES

Reconstitution and functional characterization of ion channels from nanodiscs in lipid bilayers

Laura-Marie Winterstein[1*], Kerri Kukovetz[1*], Oliver Rauh[1*], Daniel L. Turman[3], Christian Braun[1], Anna Moroni[2], Indra Schroeder[1], and Gerhard Thiel[1]

Recent studies have shown that membrane proteins can be efficiently synthesized in vitro before spontaneously inserting into soluble nanoscale lipid bilayers called nanodiscs (NDs). In this paper, we present experimental details that allow a combination of in vitro translation of ion channels into commercially available NDs followed by their direct reconstitution from these nanobilayers into standard bilayer setups for electrophysiological characterization. We present data showing that two model K^+ channels, Kcv and KcsA, as well as a recently discovered dual-topology F^- channel, Fluc, can be reliably reconstituted from different types of NDs into bilayers without contamination from the in vitro translation cocktail. The functional properties of Kcv and KcsA were characterized electrophysiologically and exhibited sensitivity to the lipid composition of the target DPhPC bilayer, suggesting that the channel proteins were fully exposed to the target membrane and were no longer surrounded by the lipid/protein scaffold. The single-channel properties of the three tested channels are compatible with studies from recordings of the same proteins in other expression systems. Altogether, the data show that synthesis of ion channels into NDs and their subsequent reconstitution into conventional bilayers provide a fast and reliable method for functional analysis of ion channels.

Introduction

Ion channels are protein tunnels, which conduct a regulated and selective transport of ions across cell membranes (Hille, 2001). Because this function is essential for many aspects of cellular life, structure/function correlates of channel proteins are intensively studied (Kurachi and North, 2004; Catterall et al., 2017). For the same reason, channels are also considered major targets of drugs (Terstappen et al., 2010; Yu et al., 2016). The planar lipid bilayer (PLB) technique is one of the many methods that are currently used for studying channel activity and their sensitivity to the lipid environment and to drugs (Zakharian, 2013). This technique has the advantage over other electrophysiological approaches in that it allows recording of channel activity on a single-molecule level under very defined conditions (e.g., phospholipid composition and electrolyte concentrations). In recent years, many attempts were made to improve the classical method of PLBs (Montal and Mueller, 1972). This resulted, among others, in a greater mechanical stability (Tien et al., 1991; Schuster et al., 1999; Khan et al., 2016), miniaturization of the recording device (Mach et al., 2008), and the ability of using asymmetrical bilayer (Syeda et al., 2008; Iwamoto and Oiki, 2015). Bilayer recordings and their variants have also been adapted for lab-on-a-chip technologies (Kongsuphol et al., 2013), which further paved the way for a scaling up for medium and high throughput screening of channel drugs.

In all the major bilayer methods, the proteins of interest are either isolated directly from cells (Nelson et al., 1980; Hirano-Iwata et al., 2016) or expressed in heterologous systems (Tapper and George, 2003). The most frequently used heterologous system is *Escherichia coli*. In the case that a protein fails to express in bacteria, it may require an alternative expression system such as the yeast *Pichia pastoris* (Pagliuca et al., 2007). After standard purification procedures, which are, depending on the expression system, more (*P. pastoris*) or less demanding and time consuming (*E. coli*), the proteins can be reconstituted into PLBs for single-channel analysis. All these procedures are well established and have been extensively used in the past decades to study structure/function correlates of many channels. One shortcoming of this procedure is that it takes, depending on the channel, 1 wk or more from the expression in bacteria to the isolation of the channel for reconstitution in the bilayer. Another potential problem, which is occasionally encountered, concerns the purity of the protein of interest. This is particularly relevant in cases in which the yield of the channel of interest is low relative to the total amount of membrane proteins in the expression system. It

[1]Plant Membrane Biophysics, Technische Universität Darmstadt, Darmstadt, Germany; [2]Department of Biosciences and Consiglio Nazionale delle Ricerche – Istituto di Biofisica, Università degli Studi di Milano, Milano, Italy; [3]Department of Biochemistry and Howard Hughes Medical Institute, Brandeis University, Waltham, MA.

*L.-M. Winterstein, K. Kukovetz, and O. Rauh contributed equally to this paper; Correspondence to Gerhard Thiel: thiel@bio.tu-darmstadt.de.

has been reported that the protein of interest may contain contaminations, including channel proteins from the expression system (e.g., from *E. coli*), even after purification (Andersen et al., 1986; Accardi et al., 2004).

An alternative strategy to a heterologous expression is provided by recent progress in cell-free translation of proteins (Rosenberg and East, 1992; Berrier et al., 2004; Katzen et al., 2005; Syeda et al., 2008; Junge et al., 2011). A channel protein is, for this purpose, translated in vitro and reconstituted in PLBs after purification. This approach has been shown to work properly in several experiments (Rosenberg and East, 1992; Shim et al., 2007; Kovácsová et al., 2015). However, in our experience, the protein of interest is often contaminated by channels from the lysate in which the protein was synthesized, even after purification.

In this study, we show that the procedure of protein synthesis can be accelerated and that the problems of contaminations can be reduced by using a combination of in vitro translation and the recently developed nanodisc (ND) technology. These NDs are nanolipoproteins consisting of a pair of helical amphipathic scaffold proteins and a central core of lipids. In an alternative approach, the scaffold proteins are substituted by a polymer ring of styrene–maleic acid (Dörr et al., 2016). The nanoscale lipid bilayers have a well-defined diameter between ∼9 and 12 nm, which provides a stable environment for membrane proteins also in detergent-free, aqueous solutions (Bayburt and Sligar, 2010). The ND technology became rapidly popular and enabled a growing number of biochemical and structural studies on membrane proteins, including ion channels. In a few recent publications, it was already reported that ion channels could be successfully incorporated from different types of NDs for electrophysiological recordings in PLBs (Banerjee and Nimigean, 2011; Braun et al., 2014a; Dörr et al., 2016). In this study, we present experimental details for a combination of in vitro translation of ion channels into commercially available NDs and their direct reconstitution from these nanoparticles into standard bilayers as a tool for rapid and contamination-free functional studies of ion channels.

Materials and methods

Cloning and mutagenesis

For in vitro protein expression, the coding sequences of Kcv_{NTS} and KcsA were amplified via PCR and cloned into the pEXP5-CT/TOPO-vector with the pEXP5-CT/TOPO TA Expression kit (Invitrogen). To express the channel proteins in their native form, a stop codon was inserted directly upstream of the coding sequence of a 6xHis tag. The F^- channel (Fluc-Ec2) coding sequence (Stockbridge et al., 2013) from *E. coli* virulence plasmid 2 was cloned into a pET-21a vector, amplified in DH5α cells, and purified via a Qiagen miniprep kit. The KcsA gene was provided by S. Keller (University of Kaiserslautern, Kaiserslautern, Germany). The well-characterized mutation E71A (Cordero-Morales et al., 2007) was introduced by site-directed mutagenesis (Papworth et al., 1996) into the KcsA sequence to abolish inactivation.

Protein expression and purification

In vitro expression was performed according to the manufacturer's instructions of the MembraneMax (MM) HN Protein Expression kit (Invitrogen). The expression took place in the presence of different nanolipoproteins (NDs) on a shaker with 1,000 rpm at 37°C for a total of 1.5 h. For the experiments described below, we used the NDs provided with the MM expression kit (containing DMPC lipids) or MSP1D1-His discs from Cube Biotech. The latter were preassembled with DMPC, DMPG, or POPC lipids. The scaffold proteins of all used NDs were His tagged to allow the purification of channel–ND complexes via metal chelate affinity chromatography. The concentration of MSP1D1-His NDs in the reaction mixture was adjusted to 30 µM.

To purify the channel–ND complexes, the crude reaction mixture was adjusted to 400 µl with equilibration buffer (10 mM imidazole, 300 mM KCl, and 20 mM NaH_2PO_4, pH 7.4, with KOH) and subsequently loaded on an equilibrated, 0.2-ml HisPur nickel–nitrilotriacetic acid agarose spin column (Thermo Scientific). To allow the binding of the His-tagged NDs to the nickel–nitrilotriacetic acid agarose resin, the columns were incubated for 45 min at room temperature (RT) and 200 rpm on an orbital shaker. Afterward, the buffer was removed by centrifugation. To eliminate unspecific binders, the column was washed three times with 400 µl of a 20-mM imidazole solution. Finally, the His-tagged NDs were eluted in three fractions with 200 µl of a 250-mM imidazole solution. All centrifugation steps were performed at 700 *g* for 2 min. After purification, the elutions were stored at 4°C; in this way, channels remained functional for many months and even years.

Vertical lipid bilayer experiments

The vertical lipid bilayer experiments were performed on a setup from IonoVation, which is described in detail elsewhere (Bartsch et al., 2013). Two Teflon chambers, with a volume of 2.5 ml each, were separated by a 25-µm-thick Teflon foil with a central 100-µm large hole. Before the experiment, the rim of the hole was treated with ∼1 µl of a 1% hexadecane in an *n*-hexane solution. Both chambers were subsequently filled up to the lower edge of the hole with electrolyte solution before adding 35 µl of 15 mg/ml phospholipid in *n*-pentane in each side of the chamber. Bilayers were formed by a folding technique (Montal and Mueller, 1972) in which opposing monolayers were generated over the hole in the septum by elevating the buffer level of each chamber. Alternatively, the lipid bilayers were formed by using the pseudo-painting/air bubble technique (Braun et al., 2014b). Bilayers generally had a capacitance of 90–110 pF.

All measurements in this study were performed at RT (20–25°C) in pure 1,2-diphytanoyl-*sn*-glycero-3-phosphocholine (DPhPC; Avanti Polar Lipids) membranes or 1–2 mol% phosphatidylinositol 4,5-bisphosphate (PIP_2) containing DPhPC membranes and with symmetrical KCl solutions (100 mM KCl and 10 mM HEPES, pH 7.0, or 90 mM KCl and 10 mM potassium acetate, pH 4). For incorporation of channel proteins into the lipid bilayer, a small amount (∼2 µl) of the purified channel–ND conjugates was added directly below the bilayer in the trans-compartment with a bent 25-µl Hamilton syringe. Multiple channel recordings were performed with the undiluted first elution fraction. For reconstitution of single-channel proteins, the first elution fraction was diluted with a pure 250-mM imidazole solution by a factor of 10^3–10^6. After channel incorporation

in the lipid bilayer, constant voltages between 160 and –160 mV were applied. Both compartments of the bilayer chamber were connected with Ag/AgCl electrodes to the headstage of an L/M-EPC-7 patch-clamp amplifier (List-Medical). Currents were filtered with a 1-kHz, four-pole Bessel filter and digitized with a sampling frequency of 5 kHz by a 16-bit LIH 1600 A/D converter (HEKA Elektronik).

Horizontal lipid bilayer experiments

Fluc-Ec2 and monobody (Mb) S9 expression and purification and Fluc-Ec2 reconstitution into *E. coli* polar lipid extract (EPL) liposomes were completed as previously reported (Stockbridge et al., 2014; Turman and Stockbridge, 2017). The horizontal planar bilayer system (Heginbotham et al., 1999) consisted of two aqueous chambers separated by an 80-µm-thick partition crafted from overhead transparency film. A 50-µm aperture was punched into the film with a butterfly mounting pin (BioQuip Products) and smoothly shaved with a surgical razor. Application of 0.2 µl of a 10 mg/ml POPE(1-palmitoyl-2-oleoyl-*sn*-glycero-3-phosphoethanolamine)/POPG (1-palmitoyl-2-oleoyl-*sn*-glycero-3-phospho-1'-*rac*-glycerol; Avanti Polar Lipids) decane solution directly onto the aperture was completed before filling chambers with buffer. Bilayers were formed by painting the aperture with a POPE/POPG decane lipid-moistened pipette bubble. Capacitance of bilayers was consistently between 45 and 60 pF. Single channels were obtained by applying 0.5 µl of liposome suspension or ND mixture to the top chamber. After single-channel incorporation, the top chamber solution was exchanged to prevent further channel insertions. Single Fluc-Ec2 channels from MM NDs or EPL proteoliposomes were fused into 70% POPE/30% POPG PLB membranes, and recordings were collected at RT (20–23°C). Single channels were recorded at –200 mV in solutions consisting of symmetric 300 mM sodium fluoride, 15 mM 3-(*N*-morpholino) propanesulfonic acid–sodium hydroxide, pH 7.0, and 50 µg/ml BSA with the trans-chamber defined as electrical ground. For all recordings in the presence of Mb blocker, 250 nM Mb S9 was added to the cis-chamber and vigorously stirred. Recordings were collected on an Axopatch 200A amplifier at a sampling rate of 2 kHz and filtered at 1 kHz with further digital filtering after acquisition to 200 Hz for analysis as previously described (Turman et al., 2015).

Contact bubble lipid bilayer experiments

Single-channel currents were alternatively measured with the contact bubble bilayer (CBB) technique (Iwamoto and Oiki, 2015), a method for single-channel recordings in very small bilayers. Two borosilicate glass pipettes (melting point, 1.5–1.8 × 100 mm; Kimble Chase) with tip diameters of ≤30 µm were pulled with a PP-830 micropipette puller (Narishige) and filled with measuring solution (100 mM KCl and 10 mM HEPES, pH 7.0, or 90 mM KCl and 10 mM potassium acetate, pH 4). The solution in both pipettes also contained channel proteins in different NDs (MM, DMPC, DMPG, and POPC), as well as liposomes of DPhPC or DPhPC + PIP_2. We typically added 2–8 µl of a 1:10 dilution from the first elution fraction to 25 µl of the pipette solution. A low concentration of the channel–ND preparation increases the chance of single-channel recordings. The glass pipettes were mounted on micromanipulators, and their tips were immersed in a hexadecane bath. Upon applying pressure to both pipettes, small bubbles (<50 µm diameter) formed at their tips in the oil–water interface. By maneuvering the glass pipettes, the two bubbles were brought in close contact, which resulted in the formation of a small bilayer at the contact zone with a capacitance of 2–5 pF in <1 min. After bilayer formation, channel proteins from the pipette solution inserted spontaneously into the target membrane. Their activity was measured via Ag/AgCl electrodes in the pipettes with a 3900A Integrating Patch Clamp amplifier (Dagan). Currents were filtered at 1 kHz and digitized with a sampling frequency of 10 kHz by an Instrutech LIH 8+8 data acquisition system A/D converter (HEKA Elektronik).

Liposome preparation

To produce liposomes, 15 mg DPhPC or DPhPC + PIP_2 (Avanti Polar Lipids) were solubilized in 1 ml chloroform (AppliChem), dried in a glass vial, and finally resuspended in 10 ml of measuring solution. Subsequently, the lipid solution was sonicated at RT for a minimum of 1 h until it was transparent. After liposome preparation, the solution was frozen in 50-µl aliquots and thawed for further use.

Ion channel recordings, data analysis, and statistics

After insertion of an active channel into the bilayer, the membrane was routinely clamped for periods between 5 s and 1 min to a range of positive and negative voltages (usually from 160 to –160 mV in 20-mV steps). Data analysis was performed with KielPatch (version 3.20 ZBM/2011) and Patchmaster (HEKA Electronik). The open probability for Kcv and KcsA was calculated with KielPatch for each voltage step and was analyzed by dividing the amount of the time that the channel was in its open state by the total length of the applied voltage protocol step. Data are presented as arithmetic mean ± SD or as geometric mean ± geometric SD of *n* independent bilayer recordings.

Online supplemental material

The supplemental material contains data on Kcv_{NTS} function that are not depicted in Fig. 1. Fig. S1 shows mean I/V relation and P_o/V relation of Kcv_{NTS} channel translated in vitro into MM NDs or NDs with DMPC, DMPG, or POPC membrane and recorded in PLBs.

Results and discussion

We tested the combination of in vitro translation of channel proteins into NDs and their functional reconstitution from the NDs into two different types of bilayers. For this purpose, the small viral channel Kcv_{NTS} (Braun et al., 2014b) was expressed in vitro into four different NDs. Three of these NDs differed in the lipids (DMPC, DMPG, and POPC), which make up the discs (source membrane). The fourth type is a frequently used commercial ND with an unknown His-tagged protein scaffold that encloses a planar DMPC bilayer. After in vitro translation and purification, which took no more than a few hours, the NDs were added directly to a lipid bilayer (target membrane) for single-channel recordings. Channels were recorded with a conventional PLB setup and alternatively in so-called CBBs. In the latter case, the

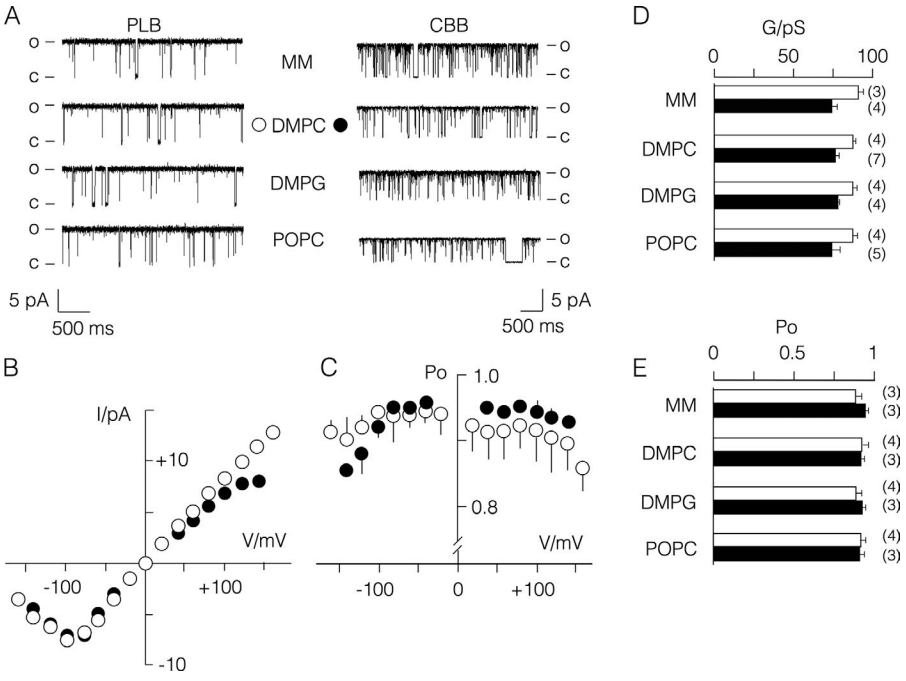

Figure 1. **Functional reconstitution of Kcv channel from different NDs in two alternative bilayer systems. (A)** Exemplary current traces of Kcv_{NTS} channel at 100 mV recorded in symmetrical KCl (100 mM, pH 7) in vertical PLB or in CBB. The channel protein was translated in vitro into MM NDs or NDs with DMPC, DMPG, or POPC membranes. The purified NDs were in a 1:1,000 or 1:10 dilution with imidazole directly administered to the bilayers or CBB, respectively. The open (o) and closed (c) levels of the channel are indicated. **(B and C)** Mean I/V relations (B) and open probability/voltage (P_o/V) relations (C) from Kcv_{NTS} channel produced in NDs with DMPC (n = 4) membranes. Symbols in B and C cross-reference to symbols in A. **(D and E)** Mean slope conductance between ±60 mV (D) and mean P_o between ±160 mV (E) for the channel recorded with PLB (open bars) or CBB (closed bars) method. Data are means ± SD; n given as numbers in parentheses.

NDs were added to the pipette solution, which was used to form CBBs. The exemplary current traces recorded at 100 mV in Fig. 1 show that the same kind of channel fluctuations were measured with both bilayer methods and from all ND preparations. None of the >100 experiments were ever contaminated with activity from another channel. Representative for all the different conditions, Fig. 1 (B and C) shows the mean I/V relations and the P_o/V relations for the channel in NDs with DMPC as a source membrane. The overall characteristics of the I/V and P_o/V relations are similar in the two recording conditions. A closer scrutiny of the data only shows that the unitary conductance of Kcv_{NTS} is independent of the type of ND and consistently smaller in CBB compared with PLB recordings (Fig. 1, B and D). Overall, the I/V and P_o/V relations obtained under the variable conditions are also similar to those from previous studies in which the same channel was expressed and purified from *P. pastoris* and reconstituted in PLBs (Braun et al., 2014a). The larger voltage window, which was tested here, only highlights the pronounced negative slope conductance at hyperpolarizing voltages, which is typical for this type of channel (Gazzarrini et al., 2009).

Comparison of the current traces (Fig. 1 A) and a detailed analysis of its activity confirm that the channel exhibits the same functional features independent of the type of ND into which it was produced. This includes the unitary conductance (Fig. 1 D), open probability (Fig. 1 E), and the overall shape of the I/V and P_o/V relations (Fig. S1). The results of these experiments confirm that NDs with channel proteins can be added directly to bilayers and that the channel proteins insert spontaneously in the final target membrane. The functional properties of the channel are largely unaffected by the type of lipid that is used for making the ND source membranes and the type of method with which channel activity is recorded (Fig. 1).

In the next experiment, we addressed the question of whether only the channel protein becomes exposed to the target bilayer or whether the ND remains intact in the target bilayer. In the first case, the channel property should be sensitive to the bilayer of the target membrane, whereas it should be insensitive in the latter case. To answer this question, we produced Kcv_{NTS} in four different NDs and reconstituted the channel in a planar DPhPC lipid bilayer with or without 1 mol% PIP_2. The exemplary current traces at 160 mV in Fig. 2 A show that the presence of PIP_2 resulted in a strong reduction of the unitary conductance. This effect, which is not further analyzed here, was voltage dependent and increased with positive voltages (Fig. 2 B). The results of these experiments show that the channel function depends on the bilayer composition of the target membrane. Hence, the channel must be exposed to the target lipid. It is reasonable to speculate that the ND at some point disintegrates and that the lipids, which surround the channel, are no longer dominated by those from the ND.

In the next step, we tested whether the combination of protein synthesis and reconstitution of the channel protein into the target membrane is affected by the flavor of the lipids in the source membrane. For this purpose, we used the same preparations that were used in Fig. 1. The respective NDs were added at a high concentration (2 µl of the undiluted elution) to a vertical DPhPC bilayer, and the insertion of the channel in the target bilayer was continuously monitored. Fig. 3 shows an example in which NDs were added at time 0 to a bilayer kept at 60 mV. After a few seconds, the first channel activity could be registered. To compare different experiments, we measured the time it took before 10 channels (= 50 pA) were active in the bilayer. In the present example, it took <1 min before this threshold was achieved. A comparison between different NDs shows that the channels inserted quickly into the target membrane when they were in NDs with DMPC or DMPG. When the channels were in NDs with a POPC bilayer, the insertion was less efficient. The results of these experiments suggest that NDs with DMPC membrane are the

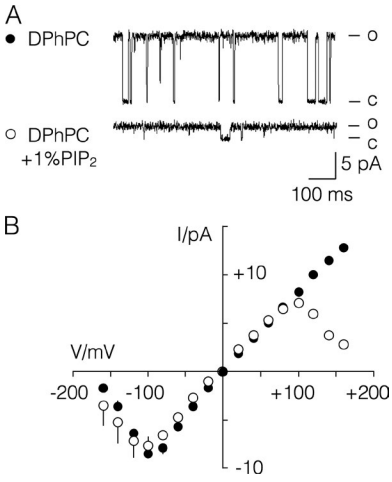

Figure 2. **The character of the target membrane determines channel function. (A)** Typical fluctuations of Kcv_{NTS} channel at 160 mV measured in PLB setup after reconstituting the protein from an MM ND into a DPhPC membrane without or with 1 mol% PIP_2. **(B)** Mean I/V relation (±SD) of Kcv_{NTS} channel from recordings as in A without (closed circles; *n* = 4) or with 1 mol% PIP_2 (open circles; *n* = 3).

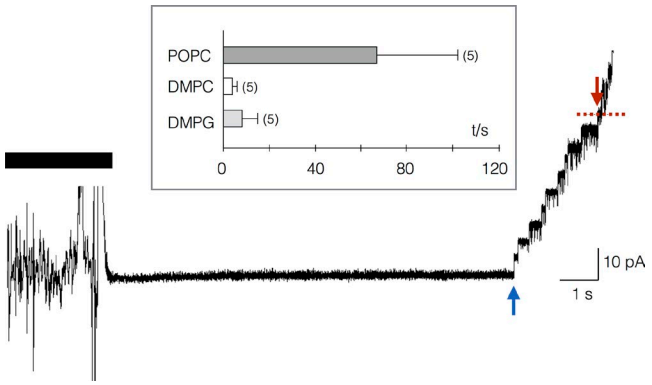

Figure 3. **Efficiency of channel reconstitution of Kcv_{NTS} from diverse NDs.** Exemplary recording of Kcv_{NTS} channel insertion from DMPC NDs into a DPhPC bilayer in PLB setup. The protein was added to the membrane held at 60 mV during the time indicated by the solid bar. After a short period of time, channels were incorporated into the bilayer. The blue and red arrows mark the difference between the baseline at the instance of the first channel insertion (blue arrow) and the insertion of 10 channels (red arrow). Inset: mean time (±SD; *n* given as numbers in parentheses) between insertion of 1st and 10th channel for reconstituting Kcv_{NTS} from NDs with POPC, DMPC, or DMPG membrane.

most suitable for functional reconstitution of the Kcv_{NTS} channel in PLBs. At this point, we cannot answer the question of whether the lipid of the source ND supports protein synthesis into the ND or the transfer from the ND to the target membrane.

In the course of the experiments, we realized that the efficiency of functional channel reconstitution progressively decreased after storing the channel-containing NDs in measuring buffer. To examine this phenomenon systematically, we collected the first fraction from an in vitro synthesis/purification of Kcv_{NTS} into MM NDs and diluted it 1:100 in 250 mM imidazole or 1:100 in measuring buffer (100 mM KCl and 10 mM HEPES, pH 7). 1 d later, the reconstitution efficiencies of both preparations were estimated. Fig. 4 A shows two representative examples in which the ND–channel stored in imidazole or in buffer were added to the bilayer. In both cases, the channels inserted into the bilayer. However, the efficiency of insertion, which was estimated from the current amplitude 1 min after the first channel had inserted into the bilayer, was on average ∼10 times lower for protein stored in measuring buffer.

To further examine this negative effect of the saline buffer on the channel, we performed experiments in which the channel was, during the course of the purification, exposed to different wash and elution buffers (Fig. 4 B). The first elution fraction was then added directly to the bilayer to examine the reconstitution efficiency. The data show that the highest efficiency was obtained when the protein was washed and eluted in a pure imidazole solution. The presence of PBS (300 mM KCl and 20 mM NaH_2PO_4, pH 7.4) in the wash buffer decreased the reconstitution efficiency. A reasonable explanation for this result is that salts in the buffer may remove NDs from the column and hence decrease the protein yield in the final preparation. The data also show that the presence of PBS in the elution buffer had no appreciable effect on the reconstitution efficiency (Fig. 4 B). The results of these experiments suggest that ions in the elution buffer have no immediate negative effect on channel insertion and/or function.

During storage in an ionic buffer, the NDs must undergo some sort of denaturation or aggregation of NDs. This effect is more augmented by the absence of imidazole than by the presence of ions. Imidazole occurs to have a stabilizing effect on the isolated ND–channel preparation. The negative effect of ions seems to become relevant already during the course of an experiment. We routinely found that we had to progressively increase the amount of NDs, which were required for a successful recording of channel activity, over a period of 3–4 h.

To obtain more information on storing ND–channel preparations, we synthesized the Kcv_{NTS} channel as in Fig. 1. The isolated NDs were then split into two batches, of which one was frozen at −20°C and the other stored at 4°C. 4 d later, both preparations were used on the same day for reconstitution in a DPhPC bilayer. The representative recordings from three experiments in Fig. 4 C show that the batch, which had been frozen for storage, failed to generate any channel activity in the bilayer. However, the second aliquot, which was stored in the refrigerator, generated reliable channel fluctuations. In other experiments, we found that a preparation kept for 3 yr at 4°C was still generating channel activity in these assays. The results of these experiments imply that ND–channel preparations are very stable when stored at 4°C but may lose activity as a result of freezing. Similar results were obtained with the Fluc-Ec2 channel (see below). Also, this protein could be stored after synthesis into NDs at 4°C but not at −80°C without compromising activity. Collectively, these data suggest that ND–channel preparations are best stored at 4°C even though freezing may not be detrimental for all types of ND–channel preparations. It has been reported that the integrity of the KcsA channel in NDs is neither compromised by freezing/thawing nor by lyophilization (Dörr et al., 2016).

The experiments in Fig. 4 (A and B) indicate that it is possible to measure very large currents after adding high amounts of active channels to the bilayer. This is remarkable because

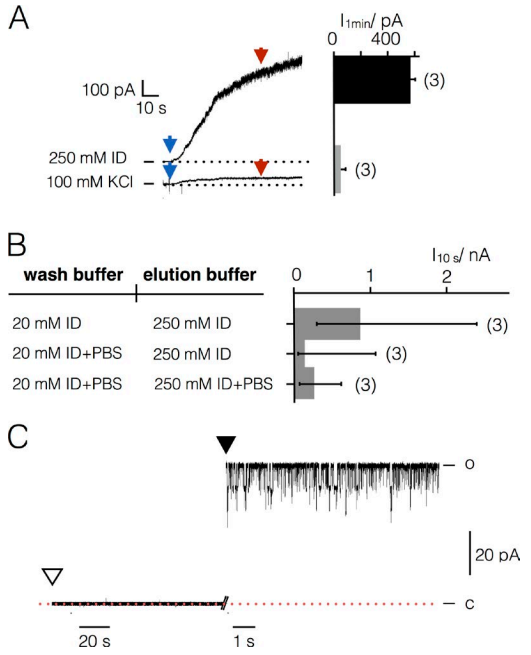

Figure 4. **Efficiency of channel reconstitution depends on preparation. (A)** Exemplary recording of channel insertion from MM NDs into DPhPC membrane in PLB setup as in Fig. 1. The Kcv_{NTS}/ND preparations were before reconstitution stored at 1:100 dilution overnight in either 250 mM imidazole or in 100 mM KCl. The preparation was added to a membrane kept at 60 mV; subsequent channel insertion was quantified by measuring the current between insertion of first channel (blue arrows) and 1 min later (red arrows). Bars on the right show mean current (±SD; *n* = 3) after 1 min as in left panel for reconstitution of NDs stored in 250 mM imidazole (black) or 100 mM KCl (gray). **(B)** Reconstitution efficiency of isolated MM NDs with Kcv_{NTS} channel. The proteins were washed and eluted during preparation with imidazole and/or PBS as indicated on the left. The undiluted first elution was added directly to bilayer as in A. The reconstitution efficiency (geometric mean ± geometric SD; *n* in parentheses) was estimated as in A over a period of 10 s after appearance of the first channel. **(C)** Exemplary reconstitution of Kcv_{NTS} in MM NDs after storing at either −20°C or 4°C. Continuous current recording of DPhPC bilayer in a vertical PLB set up after addition of Kcv_{NTS}/ND preparations (1:100 dilution) from an aliquot stored at −20°C (open triangle) or 4°C (closed triangle). Recordings start ∼10 s after addition of proteins. Red line indicates zero current level.

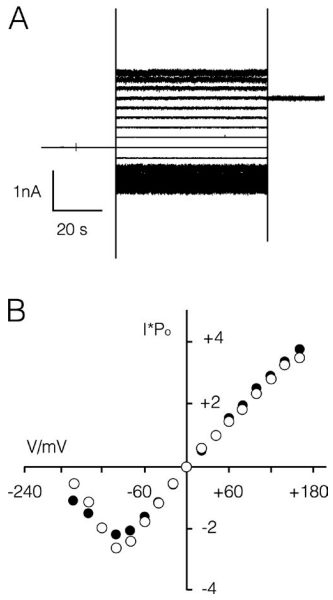

Figure 5. **Reconstitution of Kcv_{NTS} channel from NDs allows recordings of macroscopic currents in PLBs. (A)** Exemplary macroscopic Kcv_{NTS} currents elicited by voltage steps between ±160 mV. The protein was synthesized into MM NDs as in Fig. 1, and the 1:100 dilution of the first elution of the purification was added directly to the bilayer as in Fig. 4. **(B)** I/V relation of the steady-state current collected at the end of the voltage pulse (open circles) and time-averaged I/V relation (closed circles) obtained by multiplying unitary I/V relation and open probability of the same channel in Fig. 1. For comparison, both I/V relations were normalized to current at 40 mV. Currents were recorded in symmetrical buffer (100 mM KCl and 10 mM HEPES, pH 7); the membrane was clamped from a holding voltage at 0 mV for 60 s to test voltages between ±160 mV in 20-mV increments and finally for 60 s to a common postvoltage at 100 mV.

host bilayers generally tend to become unstable and burst when large numbers of channel proteins are reconstituted by fusion with liposomes. Encouraged by these large currents, we tested the possibility of measuring the macroscopic I/V properties of the Kcv_{NTS} channel in a DPhPC bilayer. The protein was synthesized as in Fig. 1 into MM NDs and added at high concentration (1:100 dilution of the first elution in pure 250 mM imidazole) to a DPhPC bilayer. In these types of experiments, we were able to measure macroscopic currents in the nanoampere range (Fig. 5 A). Worth noting is that the amplitudes of the currents were more limited by the amplifier than by the stability of the bilayer. The normalized steady-state I/V curve of the exemplary experiment in Fig. 5 A is plotted in Fig. 5 B. Note that the shape of the I/V curve with the pronounced negative slope at negative clamp voltages is the same as that of the unitary channel I/V relation (Fig. 1 B). The macroscopic I/V relation can be well reconstituted from a time-averaged I/V relation in which the unitary conductance is multiplied with the open probability of the channel from data in Fig. 1 C. Worth noting in our experiments is that the macroscopic currents, including the negative slope conductance, which we recorded in the bilayer (Fig. 5, A and B), are similar to those recorded in *Xenopus laevis* oocytes, which express a closely related channel (Gazzarrini et al., 2009). This underscores that these channels are inserting with a strong directional bias into the host bilayer. The orientation of the channel in the bilayer must be the same as in a cell; the side that faces the cytosol of the cell is facing the cis-chamber in the bilayer.

Because of the high open probability of the channel at positive voltages, we can estimate that a macroscopic current of 1.25 nA at 100 mV is, in the example of Fig. 5 A, equivalent to 180 active channels in the bilayer. In similar measurements, we could record at 100 mV in a solution with 10 mM KCl currents as large as 6 nA (mean of 3.4 ± 0.5 nA) translating into ∼5,000 (2,800 ± 400) active channels in the bilayer. From these measurements, we predict that this method is also suitable for a functional reconstitution of ion channels with a small unitary conductance or even from transport proteins like pumps or anti-/symporters with a low turnover rate.

The experiments have so far shown that the small viral K^+ channels can be successfully produced in NDs and directly incorporated into bilayers for functional testing. To examine whether the method is also suitable for other channels, we performed similar experiments with a mutant of the KcsA channel ($KcsA_{E71A}$)

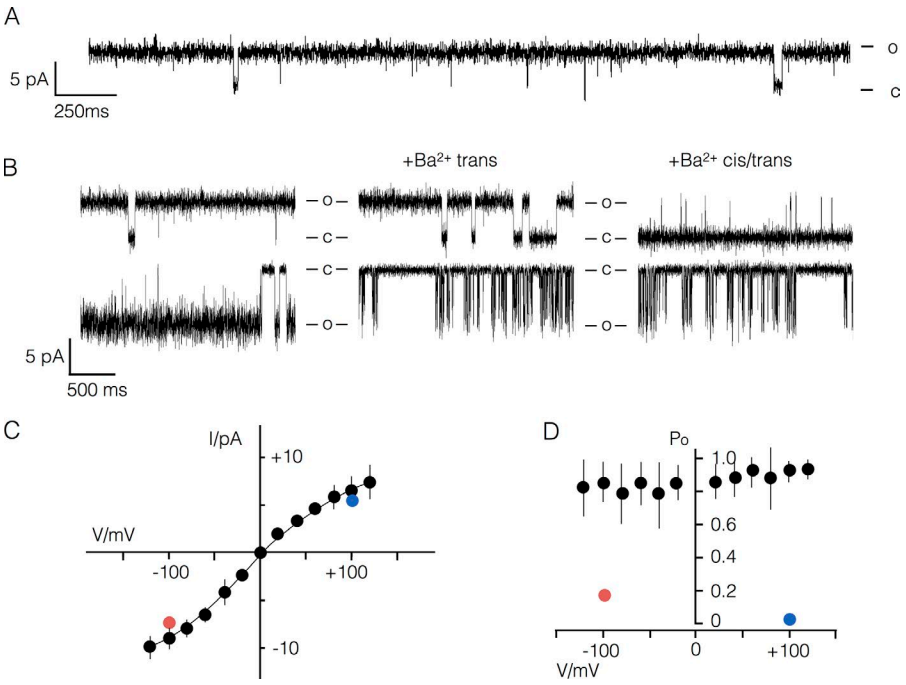

Figure 6. **Functional reconstitution of $KcsA_{E71A}$ channel in PLBs and CBBs. (A)** Exemplary current trace of $KcsA_{E71A}$ channel activity at 100 mV in symmetrical KCl (100 mM, pH 4). The channel protein was translated as in Fig. 1 in vitro into DMPC NDs and recorded in vertical PLB made from a 3:1 mix of DPhPC and DPhPS. The channel exhibits long periods with high open probability in which openings are interrupted by brief closures. **(B)** Channel fluctuations at ±100 mV in control solution before (left) and after adding 500 µM $BaCl_2$ first to the trans-chamber (middle) and then to the cis-chamber (right). **(C and D)** Unitary channel I/V relation (C) and P_0/V relation (D) from recordings of $KcsA_{E71A}$ in control solution (black circles) and after adding 500 µM $BaCl_2$ first to trans-chamber (red circles) and finally also to cis-chamber (blue circles). Data are means ± SD of $n \geq 3$ measurements.

and Fluc-Ec2 channels. KcsA is a small bacterial model channel, which provided the first crystal structure of a K^+ channel (Doyle et al., 1998). The Kcv and KcsA channels share a similar architecture with two transmembrane helixes, but KcsA has much larger cytosolic domains. The wealth of structural information has made KcsA an important model system for studying structure function relations in K^+ channels. The final channel, Fluc-Ec2, belongs to a family of dual-topology, F^--specific ion channels that protect bacteria from F^- toxicity (Ji et al., 2014). The channel is a small, 15-kD, four-pass transmembrane homodimer with antiparallel topology and two pores that are interwoven between subunits (Stockbridge et al., 2015).

The exemplary current trace in Fig. 6 A shows that $KcsA_{E71A}$ could also be successfully reconstituted from NDs into bilayers made from a 3:1 mix of DPhPC and 1,2- diphytanoyl-*sn*-glycero-3-phospho-L-serine (DPhPS). This noninactivating KcsA mutant (Cordero-Morales et al., 2006) shows its typical gating in which the channel exhibits long periods of high open probability (Fig. 6 A). The same behavior has been reported in previous experiments in which $KcsA_{E71A}$ was expressed and purified from *E. coli* and reconstituted via liposomes (Cordero-Morales et al., 2006) or nanoscaled apolipoprotein-bound bilayers (Banerjee and Nimigean, 2011) into planar bilayers. Under the experimental conditions, in all recordings the channel exhibited a slope conductance of ∼100 pS at 0 mV (Fig. 6 C) and an asymmetric I/V relation in which the inward conductance was ∼1.4 times higher than the outward conductance. The asymmetry of the I/V relation also suggests that $KcsA_{E71A}$ inserts into the membrane with a strong directional bias. A comparison shows that the functional parameters like unitary currents and P_0 values from the present recordings are within the experimental variability identical to those reported from other studies in which the same channel

Table 1. **Comparison of unitary channel currents and P_o values at selected voltages of Kcs_{AE71E} channel from this study with data from the literature**

Source	Mean current		Open probability		
	−100 mV	**100 mV**	**−100 mV**	**100 mV**	**40 mV**
	pA		P_o		
This study	−9.3 ± 1.3	6.5 ± 1.1	0.84 ± 0.1	0.91 ± 0.13	0.86 ± 0.11
Banerjee and Nimigean, 2011	−12 ± 1.5	7.2 ± 1	0.97 ± 0.01	0.97 ± 0.02	n.a.
Hirano et al., 2011	n.a.	n.a.	n.a.	n.a.	0.85 ± 0.2
Zhao et al., 2015	n.a.	6.5	n.a.	0.98 ± 0.01	n.a.

Kcs_{AE71E} was produced in *E. coli* (Banerjee and Nimigean, 2011; Hirano et al., 2011; Zhao et al., 2015) and reconstituted in PLBs from NDs (Banerjee and Nimigean, 2011) or via microsomes (Hirano et al., 2011; Zhao et al., 2015). In all cases, channel activity was recorded in bilayers containing anionic lipids in buffers with 100 mM K^+, pH 4.0 (Banerjee and Nimigean, 2011; Zhao et al., 2015), or 200 mM K^+, pH 4.0 (Hirano et al., 2011). Literature data were estimated from figures in respective publications. Data from this study are from Fig. 6. Information on current amplitudes or open probabilities, which is not available from the literature, is indicated by n.a. in the table.

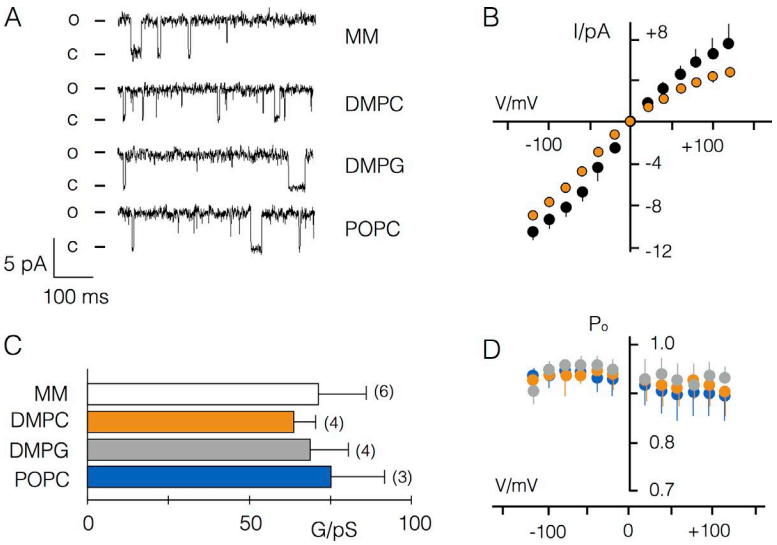

Figure 7. **Functional reconstitution of $KcsA_{E71A}$ channel in PLBs in pure DPhPC membrane. (A)** Exemplary current traces of $KcsA_{E71A}$ channel activity at 100 mV in symmetrical KCl (100 mM, pH 4). The protein was produced into MM NDs or NDs with DMPC, DMPG, or POPC membranes and reconstituted in a pure DPhPC membrane. **(B)** Mean I/V relations from $KcsA_{E71A}$ channel produced in DMPC NDs and reconstituted in pure DPhPC bilayers (orange circles) or in bilayers made of a 3:1 mix of DPhPC and DPhPS (data from Fig. 6). **(C)** Mean slope conductance (±SD, *n* given as number of experiments in parentheses) between ±40 mV for $KcsA_{E71A}$ channel reconstituted from different NDs into pure DPhPC membranes in vertical PLBs from pure DPhPC. **(D)** P_O/V relation of $KcsA_{E71A}$ synthesized into NDs with different lipids and reconstituted into pure DPhPC membranes in vertical PLBs. Color of symbols in C cross-references with data in D.

was synthesized and/or reconstituted in PLBs by different methods (Table 1).

To further test whether the KcsA protein also exhibits its characteristic functional features after reconstitution from NDs, we examined its sensitivity to Ba^{2+}. In classical bilayer studies, it has been shown that the KcsA wild-type channel ($KcsA_{wt}$) is blocked in a nonsymmetrical manner by Ba^{2+} (Piasta et al., 2011). Fig. 6 B shows recordings from an experiment in which Ba^{2+} was first added at 500 µM to the trans-, and in a second step, to the cis-chamber. The current traces and I/V data (Fig. 6, B and C) are in agreement with previous measurements with $KcsA_{E71A}$ (Banerjee and Nimigean, 2011) that the channel exhibits in the presence of Ba^{2+} still full openings. The lifetime of these events is, however, dramatically shortened in the presence of Ba^{2+} compared with the control. It is also evident that the Ba^{2+} effect is stronger when the blocker is added to the cis- rather than to the trans-side. On average, 500 µM Ba^{2+} reduced in three experiments P_o at −100 mV and 100 mV to 23% and 1% when added to the trans- and cis-side, respectively (Fig. 6 D). In all these functional aspects (e.g., Ba^{2+}-induced reduction of the open lifetime and nonsymmetrical sensitivity to the blocker), the $KcsA_{E71A}$ channel reconstituted from NDs behaves in the same manner as reported from previous experiments in which $KcsA_{wt}$ was recorded in classical bilayer experiments.

It has been reported that the $KcsA_{wt}$ channel requires anionic phospholipids in the bilayer for function (Valiyaveetil et al., 2002). This dependency provides another test for the question of whether the channel is, after insertion, fully exposed to the phospholipids of the target bilayer or remains under the influence of lipids from the NDs into which it was synthesized. To address this question, $KcsA_{E71A}$ was synthesized into NDs with different phospholipids, of which one was made of the anionic phospholipid DMPG. The channels were then reconstituted into a pure DPhPC bilayer. In all cases, this resulted in measurable $KcsA_{E71A}$ activity (Fig. 7). The unitary I/V relations were nonsymmetrical as in the case of a reconstitution into the DPhPC/DPhPS bilayer. However, worth noting is that the unitary conductance was, in the absence of the anionic lipid, significantly lower than in the mixed DPhPC/DPhPS bilayer (Fig. 7 B). This reflects the known sensitivity of the unitary conductance of Kcv_{wt} on anionic lipids (Marius et al., 2008). The open probability of the KcsA channel was also in a pure DPhPC bilayer high (Fig. 7 D) and independent on the phospholipid of the source bilayer. The results of these experiments have several implications; first, they suggest that an anionic lipid is not mandatory for $KcsA_{E71A}$ activity. This result is in agreement with the observations of others who also observed activity of the $KcsA_{wt}$ channel in the absence of anionic phospholipids (Rotem et al., 2010; McGuire and Blunck, 2015). Second, the effect of the anionic lipid in the target bilayer on the unitary conductance confirms the data from Fig. 2 in that the protein is, after insertion, fully exposed to the phospholipids of the target bilayer. Finally, anionic phospholipids, which may remain associated with the channel protein (Valiyaveetil et al., 2002), e.g., from the ND lipid, have no obvious influence on channel gating and conductance. Collectively, the data suggest that the dependency of KcsA activity on anionic lipids may be more related to the insertion of the protein into liposomes or the transfer from the liposomes into the target membrane.

The Fluc-Ec2 ion channel is a topologically unusual system for in vitro translation and reconstitution into NDs. This topology requires that each monomer of the homodimer inserts in the opposite direction relative to its neighbor within the ND during in vitro translation. As Fig. 8 attests, using single-channel PLB recordings as a functional indicator, channels from an in vitro synthesis reconstituted into MM NDs are indistinguishable from channels expressed in *E. coli* and reconstituted in a traditional EPL proteoliposome system. A general overview of the channels in Fig. 8 A (top) shows the functional characteristics of Fluc-Ec2 single channels, such as brief, millisecond closings and short-lived subconducting states that are the same in both reconstitution methods (Stockbridge et al., 2013). Fig. 8 A (bottom) shows discrete, seconds-long, full-blocking events from a highly specific Mb blocker, S9, confirming that the channels from the MM ND reconstitution are properly folded and have the specific epitope required for Mb block available (Stockbridge et al., 2015; Turman et al., 2015; Turman and Stockbridge, 2017). Moreover, the open probabilities (Fig. 8 B) of the unblocked channels are 0.99 ± 0.002 ($n = 3$) as previously noted (Stockbridge et al., 2013). In the presence of 250 nM Mb S9, the open probabilities are 0.29

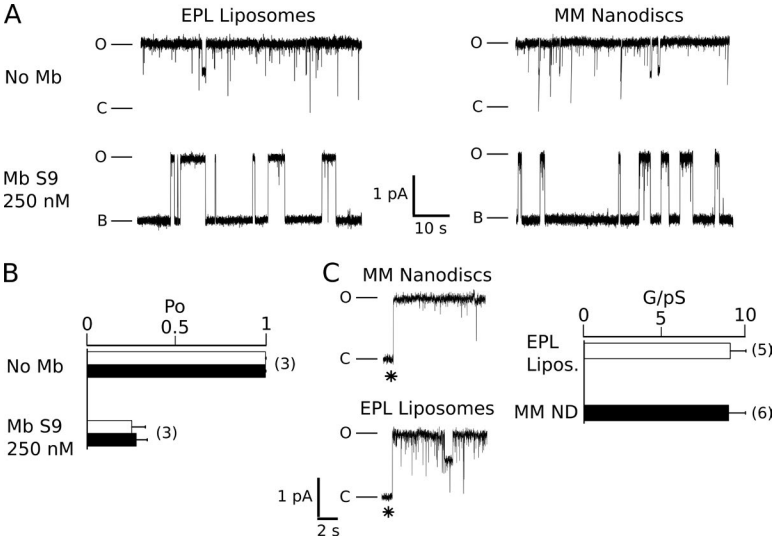

Figure 8. **Comparison of Fluc-Ec2 functional reconstitution in EPL liposomes and MM NDs. (A)** Representative single-channel recordings in the absence (top) and presence of 250 nM Mb S9 blocker (bottom) in POPE/POPG PLB membranes. Left: Single Fluc-Ec2 channels reconstituted in EPL liposomes. Right: Single Fluc-Ec2 channels reconstituted in MM NDs. Open (O), closed (C), and blocked (B) conductance levels indicated on left of traces. **(B)** Open probabilities of single Fluc-Ec2 channels with and without Mb S9 reconstituted in MM NDs (open bars) and EPL liposomes (closed bars). **(C)** Left: Single-channel insertion events denoted by asterisks from MM NDs (top) and EPL liposomes (bottom). Right: Single Fluc-Ec2 channel conductance measured from insertion events.

± 0.04 ($n = 3$) as expected for a blocker with an affinity of 120 nM (Stockbridge et al., 2014). In Fig. 8 C, the unitary conductance measured from single-channel insertion events is also the same between both reconstitution methods. This single pot in vitro synthesis and reconstitution method is an efficient technological breakthrough in the functional study of the Fluc-Ec2 system.

Conclusion

These experiments show that different types of K^+ channels and an F^- channel can be easily synthesized in vitro into NDs. After purification via a His tag on the scaffold protein, which surrounds the lipid ND, the channels can then be efficiently reconstituted directly from the NDs into conventional bilayers for functional characterization. The entire procedure takes no longer than a few hours. The efficiency of channel reconstitution depends on the lipids in the NDs and on the buffer in which the preparations are stored. This suggests that the method can be optimized for each channel of interest. The functional properties of the reconstituted channels are sensitive to the lipid composition of the target bilayer, suggesting that the proteins are fully immersed into the target membrane. The basic functional properties of the tested channels are similar to those reported from measurements of the same channels with other methods. This combination of reliable and reproducible channel function with the short time for channel synthesis and purification, as well as the absence of contaminations from other channels, makes this procedure a very versatile method for a functional reconstitution of the ion channel in bilayers.

Acknowledgments

We thank Professor Sandro Keller for the KcsA clone.

This research was supported by the H2020 European Research Council NoMAGIC grant (awarded to A. Moroni and G. Thiel), the LOEWE initiative iNAPO (to G. Thiel), the Deutsche Forschungsgemeinschaft SCHR1467/1-1 (to I. Schroeder), Ministero Affari Esteri e Cooperazione Internazionale PGR00139, Fondazione Cariplo grant 2014-0660 (to A. Moroni), and the Howard Hughes Medical Institute grant RO1-GM107023 (to D.L. Turman).

The authors declare no competing financial interests.

Author contributions: C. Braun established the method. L.-M. Winterstein, K. Kukovetz, O. Rauh, and D.L. Turman performed experiments, analyzed data, and wrote parts of the paper. I. Schroeder, A. Moroni, and G. Thiel designed the work and wrote the paper.

Kenton J. Swartz served as editor.

Submitted: 15 September 2017
Revised: 20 December 2017
Accepted: 30 January 2018

References

Accardi, A., L. Kolmakova-Partensky, C. Williams, and C. Miller. 2004. Ionic currents mediated by a prokaryotic homologue of CLC Cl^- channels. *J. Gen. Physiol.* 123:109–119. https://doi.org/10.1085/jgp.200308935

Andersen, O.S., W.N. Green, and B.W. Urban. 1986. Ion conduction through sodium channels in planar lipid bilayers. *In* Ion Channel Reconstitution. C. Miller, editor. Plenum Press, New York. 385–404. https://doi.org/10.1007/978-1-4757-1361-9_15

Banerjee, S., and C.M. Nimigean. 2011. Non-vesicular transfer of membrane proteins from nanoparticles to lipid bilayers. *J. Gen. Physiol.* 137:217–223. https://doi.org/10.1085/jgp.201010558

Bartsch, P., A. Harsman, and R. Wagner. 2013. Single channel analysis of membrane proteins in artificial bilayer membranes. *Methods Mol. Biol.* 1033:345–361. https://doi.org/10.1007/978-1-62703-487-6_22

Bayburt, T.H., and S.G. Sligar. 2010. Membrane protein assembly into Nanodiscs. *FEBS Lett.* 584:1721–1727. https://doi.org/10.1016/j.febslet.2009.10.024

Berrier, C., K.-H. Park, S. Abes, A. Bibonne, J.M. Betton, and A. Ghazi. 2004. Cell-free synthesis of a functional ion channel in the absence of a membrane and in the presence of detergent. *Biochemistry.* 43:12585–12591. https://doi.org/10.1021/bi049049y

Braun, C.J., T. Baer, A. Moroni, and G. Thiel. 2014b. Pseudo painting/air bubble technique for planar lipid bilayers. *J. Neurosci. Methods.* 233:13–17. https://doi.org/10.1016/j.jneumeth.2014.05.031

Braun, C.J., C. Lachnit, P. Becker, L.M. Henkes, C. Arrigoni, S.M. Kast, A. Moroni, G. Thiel, and I. Schroeder. 2014a. Viral potassium channels as a robust model system for studies of membrane-protein interaction. *Biochim. Biophys. Acta.* 1838:1096–1103. https://doi.org/10.1016/j.bbamem.2013.06.010

Catterall, W.A., G. Wisedchaisri, and N. Zheng. 2017. The chemical basis for electrical signaling. *Nat. Chem. Biol.* 13:455–463. https://doi.org/10.1038/nchembio.2353

Cordero-Morales, J.F., L.G. Cuello, Y. Zhao, V. Jogini, D.M. Cortes, B. Roux, and E. Perozo. 2006. Molecular determinants of gating at the potassium-channel selectivity filter. *Nat. Struct. Mol. Biol.* 13:311–318. https://doi.org/10.1038/nsmb1069

Cordero-Morales, J.F., V. Jogini, A. Lewis, V. Vásquez, D.M. Cortes, B. Roux, and E. Perozo. 2007. Molecular driving forces determining potassium channel slow inactivation. *Nat. Struct. Mol. Biol.* 14:1062–1069. https://doi.org/10.1038/nsmb1309

Dörr, J.M., S. Scheidelaar, M.C. Koorengevel, J.J. Dominguez, M. Schäfer, C.A. van Walree, and J.A. Killian. 2016. The styrene-maleic acid copolymer: a versatile tool in membrane research. *Eur. Biophys. J.* 45:3–21. https://doi.org/10.1007/s00249-015-1093-y

Doyle, D.A., J. Morais Cabral, R.A. Pfuetzner, A. Kuo, J.M. Gulbis, S.L. Cohen, B.T. Chait, and R. MacKinnon. 1998. The structure of the potassium channel: molecular basis of K^+ conduction and selectivity. *Science.* 280:69–77. https://doi.org/10.1126/science.280.5360.69

Gazzarrini, S., M. Kang, A. Abenavoli, G. Romani, C. Olivari, D. Gaslini, G. Ferrara, J.L. van Etten, M. Kreim, S.M. Kast, et al. 2009. Chlorella virus ATCV-1 encodes a functional potassium channel of 82 amino acids. *Biochem. J.* 420:295–303. https://doi.org/10.1042/BJ20090095

Heginbotham, L., M. LeMasurier, L. Kolmakova-Partensky, and C. Miller. 1999. Single *streptomyces lividans* K^+ channels: functional asymmetries and sidedness of proton activation. *J. Gen. Physiol.* 114:551–560. https://doi.org/10.1085/jgp.114.4.551

Hille, B. 2001. Ion Channels of Excitable Membranes. Third edition. Sinauer Associates Inc., Sunderland. 814 pp.

Hirano, M., Y. Onishi, T. Yanagida, and T. Ide. 2011. Role of the KcsA channel cytoplasmic domain in pH-dependent gating. *Biophys. J.* 101:2157–2162. https://doi.org/10.1016/j.bpj.2011.09.024

Hirano-Iwata, A., Y. Ishinari, M. Yoshida, S. Araki, D. Tadaki, R. Miyata, K. Ishibashi, H. Yamamoto, Y. Kimura, and M. Niwano. 2016. Reconstitution of Human Ion Channels into Solvent-free Lipid Bilayers Enhanced by Centrifugal Forces. *Biophys. J.* 110:2207–2215. https://doi.org/10.1016/j.bpj.2016.04.010

Iwamoto, M., and S. Oiki. 2015. Contact bubble bilayers with flush drainage. *Sci. Rep.* 5:9110. https://doi.org/10.1038/srep09110

Ji, C., R.B. Stockbridge, and C. Miller. 2014. Bacterial fluoride resistance, Fluc channels, and the weak acid accumulation effect. *J. Gen. Physiol.* 144:257–261. https://doi.org/10.1085/jgp.201411243

Junge, F., S. Haberstock, C. Roos, S. Stefer, D. Proverbio, V. Dötsch, and F. Bernhard. 2011. Advances in cell-free protein synthesis for the functional and structural analysis of membrane proteins. *N. Biotechnol.* 28:262–271. https://doi.org/10.1016/j.nbt.2010.07.002

Katzen, F., G. Chang, and W. Kudlicki. 2005. The past, present and future of cell-free protein synthesis. *Trends Biotechnol.* 23:150–156. https://doi.org/10.1016/j.tibtech.2005.01.003

Khan, M.S., N.S. Dosoky, B.K. Berdiev, and J.D. Williams. 2016. Electrochemical impedance spectroscopy for black lipid membranes fused with channel protein supported on solid-state nanopore. *Eur. Biophys. J.* 45:843–852. https://doi.org/10.1007/s00249-016-1156-8

Kongsuphol, P., K.B. Fang, and Z. Ding. 2013. Lipid bilayer technologies in ion channel recordings and their potential in drug screening assay. *Sens. Actuators B Chem.* 185:530–542. https://doi.org/10.1016/j.snb.2013.04.119

Kovácsová, G., E. Gustavsson, J. Wang, M. Kreir, S. Peuker, and S. Westenhoff. 2015. Cell-free expression of a functional pore-only sodium channel. *Protein Expr. Purif.* 111:42–47. https://doi.org/10.1016/j.pep.2015.03.002

Kurachi, Y., and A. North. 2004. Ion channels: their structure, function and control – an overview. *J. Physiol.* 554:245–247. https://doi.org/10.1113/jphysiol.2003.057703

Mach, T., C. Chimerel, J. Fritz, N. Fertig, M. Winterhalter, and C. Fütterer. 2008. Miniaturized planar lipid bilayer: increased stability, low electric noise and fast fluid perfusion. *Anal. Bioanal. Chem.* 390:841–846. https://doi.org/10.1007/s00216-007-1647-7

Marius, P., M. Zagnoni, M.E. Sandison, J.M. East, H. Morgan, and A.G. Lee. 2008. Binding of anionic lipids to at least three nonannular sites on the potassium channel KcsA is required for channel opening. *Biophys. J.* 94:1689–1698. https://doi.org/10.1529/biophysj.107.117507

McGuire, H., and R. Blunck. 2015. Studying clustering of KcsA channels using single-channel voltage clamp fluorescence imaging. *Biophys. J.* 108:440a. https://doi.org/10.1016/j.bpj.2014.11.2404

Montal, M., and P. Mueller. 1972. Formation of bimolecular membranes from lipid monolayers and a study of their electrical properties. *Proc. Natl. Acad. Sci. USA.* 69:3561–3566. https://doi.org/10.1073/pnas.69.12.3561

Nelson, N., R. Anholt, J. Lindstrom, and M. Montal. 1980. Reconstitution of purified acetylcholine receptors with functional ion channels in planar lipid bilayers. *Proc. Natl. Acad. Sci. USA.* 77:3057–3061. https://doi.org/10.1073/pnas.77.5.3057

Pagliuca, C., T.A. Goetze, R. Wagner, G. Thiel, A. Moroni, and D. Parcej. 2007. Molecular properties of Kcv, a virus encoded K^+ channel. *Biochemistry.* 46:1079–1090. https://doi.org/10.1021/bi061530w

Papworth, C., J.C. Bauer, and J.C. Braman. 1996. Site-directed mutagenesis in one day with >80% efficiency. *Strategies.* 9:3–4.

Piasta, K.N., D.L. Theobald, and C. Miller. 2011. Potassium-selective block of barium permeation through single KcsA channels. *J. Gen. Physiol.* 138:421–436. https://doi.org/10.1085/jgp.201110684

Rosenberg, R.L., and J.E. East. 1992. Cell-free expression of functional Shaker potassium channels. *Nature.* 360:166–169. https://doi.org/10.1038/360166a0

Rotem, D., A. Mason, and H. Bayley. 2010. Inactivation of the KcsA potassium channel explored with heterotetramers. *J. Gen. Physiol.* 135:29–42. https://doi.org/10.1085/jgp.200910305

Schuster, B., U.B. Sleytr, A. Diederich, G. Bähr, and M. Winterhalter. 1999. Probing the stability of S-layer-supported planar lipid membranes. *Eur. Biophys. J.* 28:583–590. https://doi.org/10.1007/s002490050240

Shim, J.W., M. Yang, and L.-Q. Gu. 2007. In vitro synthesis, tetramerization and single channel characterization of virus-encoded potassium channel Kcv. *FEBS Lett.* 581:1027–1034. https://doi.org/10.1016/j.febslet.2007.02.005

Stockbridge, R.B., J.L. Robertson, L. Kolmakova-Partensky, and C. Miller. 2013. A family of fluoride-specific ion channels with dual-topology architecture. *eLife.* 2:e01084.

Stockbridge, R.B., A. Koide, C. Miller, and S. Koide. 2014. Proof of dual-topology architecture of Fluc F- channels with monobody blockers. *Nat. Commun.* 5:5120. https://doi.org/10.1038/ncomms6120

Stockbridge, R.B., L. Kolmakova-Partensky, T. Shane, A. Koide, S. Koide, C. Miller, and S. Newstead. 2015. Crystal structures of a double-barrelled fluoride ion channel. *Nature.* 525:548–551. https://doi.org/10.1038/nature14981

Syeda, R., M.A. Holden, W.L. Hwang, and H. Bayley. 2008. Screening blockers against a potassium channel with a droplet interface bilayer array. *J. Am. Chem. Soc.* 130:15543–15548. https://doi.org/10.1021/ja804968g

Tapper, A.R., and A.L. George Jr. 2003. Heterologous expression of ion channels. *Methods Mol. Biol.* 217:285–294.

Terstappen, G.C., R. Roncarati, J. Dunlop, and R. Peri. 2010. Screening technologies for ion channel drug discovery. *Future Med. Chem.* 2:715–730. https://doi.org/10.4155/fmc.10.180

Tien, H.T., Z. Salamon, and A. Ottova. 1991. Lipid bilayer-based sensors and biomolecular electronics. *Crit. Rev. Biomed. Eng.* 18:323–340.

Turman, D.L., and R.B. Stockbridge. 2017. Mechanism of single- and double-sided inhibition of dual topology fluoride channels by synthetic monobodies. *J. Gen. Physiol.* 149:511–522. https://doi.org/10.1085/jgp.201611747

Turman, D.L., J.T. Nathanson, R.B. Stockbridge, T.O. Street, and C. Miller. 2015. Two-sided block of a dual-topology F- channel. *Proc. Natl. Acad. Sci. USA.* 112:5697–5701. https://doi.org/10.1073/pnas.1505301112

Valiyaveetil, F.I., Y. Zhou, and R. MacKinnon. 2002. Lipids in the structure, folding, and function of the KcsA K^+ channel. *Biochemistry.* 41:10771–10777.

Yu, H.B., M. Li, W.P. Wang, and X.L. Wang. 2016. High throughput screening technologies for ion channels. *Acta Pharmacol. Sin.* 37:34–43. https://doi.org/10.1038/aps.2015.108

Zakharian, E. 2013. Recording of ion channel activity in planar lipid bilayer experiments. *Methods Mol. Biol.* 998:109–118. https://doi.org/10.1007/978-1-62703-351-0_8

Zhao, R., H. Dai, N. Mendelman, L.G. Cuello, J.H. Chill, and S.A. Goldstein. 2015. Designer and natural peptide toxin blockers of the KcsA potassium channel identified by phage display. *Proc. Natl. Acad. Sci. USA.* 112:E7013–E7021. https://doi.org/10.1073/pnas.1514728112